ISSN: 0975-8585

Research Journal of Pharmaceutical, Biological and Chemical Sciences

# Photovoltaic Characterization of Nano-Titania based DSSCs using Xanthene Dyes.

**Raman Kumar Saini[†], Devender Singh[†], Shri Bhagwan, Sonika, Ishwar Singh and Pratap Singh Kadyan*.**

Department of Chemistry, Maharshi Dayanand University, Rohtak, Haryana-124001, India.

**ABSTRACT**

Fabrication of dye sensitized solar cells were made by applying xanthene dyes i.e. rhodamine B and rhodamine 6G on fluorine-doped tin oxide (FTO) fused silica substrate. $TiO_2$ nanoparticles layer was used as photo anode electrode and quaternary ammonium iodide salts ($R_4N^+I^-$) and KI with iodine ($I_2$) were applied as redox electrolyte ($I^-/I_3^-$) in acetonitrile solvent. Sensitization activity of the xanthene dyes in terms of current-potential (I-V) curve, open-circuit voltage ($V_{oc}$), fill factor (FF) and overall solar energy conversion efficiency (η) were determined. Maximum efficiency (3.817) was found in rhodamine B dye with $(CH_3CH_2CH_2)_4NI$-$I_2$ redox electrolyte. Highest value of open circuit voltage ($V_{oc}$) was observed in rhodamine 6G with $(CH_3CH_2)_4NI$-$I_2$ redox electrolyte. The broad electronic absorption spectra of these dyes were found in the UV-Vis region at 341, 348 due to π→π*and 501 and 590 due to n→π*. The contribution of these dyes as light harvesting species are analysed applying photocurrent action of fabricated solar cells, which analyses that these dyes can be used for high performance in photovoltaic applications.

**Keywords:** DSSC, xanthene dyes, alkyl quaternary ammonium iodide, redox electrolyte.

[†]Contributed equally to this work

***Corresponding author***

ISSN: 0975-8585

## INTRODUCTION

Nobel laureate Richard Smalley considered environment and energy problems on the top of challenges have to face in future. The enormous demand of energy has accelerated the depletion of the earth's oil reserves and the combustion fatigue of fossil fuels which results in the environmental pollution and greenhouse effect. Due to these inescapable global challenges demand of developing more renewable energy sources, photovoltaic technologies become an area of interest in the design of solar to electrical energy conversion cells. Among all the renewable energy forms, solar energy has showed its advantages and potential for power generation. The solar energy offers a great potential due to its unrestricted and natural source of energy. Solar emit energy ~3.8 million EJ/year, which is approximately 10,000 times more than current energy needed [1]. Solar cells which absorb photon and convert into electrical energy are composed of semiconducting materials with electrical contacts and protective layers. Polycrystalline silicone (Si) is the most commonly used semiconductor, however others include single-crystal Si, the thin film materials-amorphous Si, CdTe and CuIn(Ga)$Se_2$ [2-3]. The first inorganic solar cell based on Si and developed at Bell Laboratories in 1954 had an efficiency of 6% [4]. Even though multijunction solar cell has been successfully performed in the laboratory scale with up to 40% conversion efficiency [5], but their high production cost and toxicity to environment are problem to use as solar electricity in a very large scale [6].

Solar cells based on organic dye, semiconductor and electrolyte known as dye sensitized solar cell (DSSC) and Gratzel cell [7] have the potential to compete with more mature crystalline and thin film based photovoltaic solar cell. This technology has suggested being easy manufacturing process, significantly economical and low temperatures fabrication of dye sensitized solar cell than silicon-based solar cells [7]. In the early 1960s, the conducting properties of many common dyes such as methylene blue were discovered [8] and later these dyes among the first organic materials were used to demonstrate the photovoltaic effect [9]. In the 1980s, the first polymers solar cells based on dyes or polymers yielded limited power conversion efficiencies, typically below 0.1% [10]. In 1986, the first bilayer solar cell consisting of two conjugated small molecules organic layers was reported by Tang [11]. The power conversion efficiency of about 1% was achieved in this bilayer solar cell. DSSC fabrication process involving the low temperature of deposition or printing techniques is expected to reduce the cost and boost their commercial attractiveness. In addition, the favorable attributes of dye sensitized solar cells are light weight, flexibility, and not fragile which makes them particularly suitable for transportation and portable electronics applications.

In present analysis the electronic, optical properties and photovoltaic properties of fabricated dye sensitized solar cells have been studied using organic dyes i.e rhodamine B and rhodamine 6G. The experimental studies of rhodamine B and rhodamine 6G dyes have been extensively investigated. Nanocrystalline $TiO_2$ used as photoanode in fabrication of DSSCs. The performance of fabricated DSSCs has been presented by using different electrolytes of quaternary alkyl ammonium iodide, KI/iodine ($I_2$) redox couple in acetonitrile solvent.

## MATERIAL AND METHODS

### Chemicals

Fluorine doped tin oxide (FTO) conducting glass with resistance 6-8 Ω/square was used as transparent substrate purchased from Sigma-Aldrich. The commercial product nano-titania P25 powder (Sigma-Aldrich) having 80% anatase and 20% rutile (~21 nm) size was used for preparing photoanode. Rhodamine B ([9-(2-carboxyphenyl)-6-diethylamino-3-xanthenylidene]-diethylammonium chloride) and rhodamine 6G ([9-(2-ethoxycarbonylphenyl)-6-(ethylamino)-2,7-dimethylxanthen-3-ylidene]-ethylazanium) were used as sensitizers. The acetonitrile was employed as medium of electrolytic solution; A. R. grade potassium iodide (KI), iodine ($I_2$), tetramethylquaternaryammonium iodide [$(CH_3)_4NI$], tetraethylquaternaryammonium iodide [$(CH_3CH_2)_4NI$], tetrapropylquaternaryammonium iodide [$(CH_3CH_2CH_2)_4NI$] (Sigma–Aldrich) were purchased and used as such without further purification.

### Instrumentation and measurements

Current–voltage curves were recorded by a digital Keithley 2450 source meter assembled with computer and controlled by kickstart software. Simulated light irradiation was used by a 200W tungsten (W)

arc lamp. The absorption spectra of the organic dyes were recorded by a Shimadzu 2450 spectrophotometer UV–Vis (range 180–1100 nm). TGA was performed on STA7300 from Hitachi. TGA and DTA curves were obtained by heating dyes from 35 to 500 °C at a heating rate of 10 °C/min with flow rate of 150 ml $min^{-1}$ pure nitrogen atmosphere to avoid thermal oxidation.

**Fabrication of DSSCs**

Fluorine doped Tin Oxide (FTO) glass plates were cleaned in neutral soap solution, rinsed with de-ionized water as well as with acetone and dried in ambient conditions. The cleaning of the FTO surface is an important factor governing the performance of the solar cells devices [13]. A nanocrystalline $TiO_2$ colloidal dispersion was prepared by adding 1gm of $TiO_2$ (P25 Degussa product) powder in 1 ml of glacial acetic acid. Further, 0.2 ml of acetic acid then sonicated for 15 minutes to prevent the re-aggregation of $TiO_2$ particles. A plastic adhesive tape was fixed as spacer on the four sides of conducting glass substrate (FTO) to restrict the area and thickness of $TiO_2$ film. The prepared colloidal paste of $TiO_2$ was spread over FTO substrate employing doctor blade technique to obtain a nanocrystalline layer. After the $TiO_2$ layers get dried, the films were sintered at 300°C for 2 h in oven to improve the electronic contact among particles and to burnout organic binders. The sintered $TiO_2$ layer on FTO coated transparent conducting substrate electrodes were dipped in dyes aqueous solution for 24 h at room temperature. $TiO_2$ layer were washed again with the distilled water and allowed to dry for 30 min in oven. The absorption of dyes on sintered $TiO_2$ layer was found good as shown in fig. 1. The electrolytic solutions were prepared by mixing iodine ($I_2$) (0.01M) with potassium iodide (KI) (0.1M)/ tetramethylquaternaryammonium iodide [$(CH_3)_4NI$] (0.1M)/ tetraethylquaternaryammonium iodide [$(CH_3CH_2)_4NI$] (0.1M)/ tetrapropylquaternaryammonium iodide [$(CH_3CH_2CH_2)_4NI$] (0.1M) in acetonitrile solvent. The counter electrodes were made by developing a thin film of graphite on FTO glass substrates. The counter electrode was allowed to dry at 80°C for 30 min. The DSSCs were made by clamping the photo electrode consisting of $TiO_2$ layer with absorption of dye and counter electrode then put electrolytic solution between two electrodes. The configuration of fabricated DSSCs were as: FTO (substrate)/nanocrystalline $TiO_2$ (as photoanode)/ rhodamine B or rhodamine 6G (as sensitizer)/KI or $(CH_3)_4NI$ or $(CH_3CH_2)_4NI$ or $(CH_3CH_2CH_2)_4NI$ with $I_2$ (as electrolyte) /graphite (counter electrode)/ FTO (substrate).

## RESULTS AND DISCUSSION

In the design of dye sensitized solar cells, the band gap ($E_g$) value and position of HOMO and LUMO levels of dye are the most accountable parameters. The band gap ($E_g$) of donor dye molecule helps in the expansion of the range in radiation absorption which improves the photocurrent efficiency of the dyes.

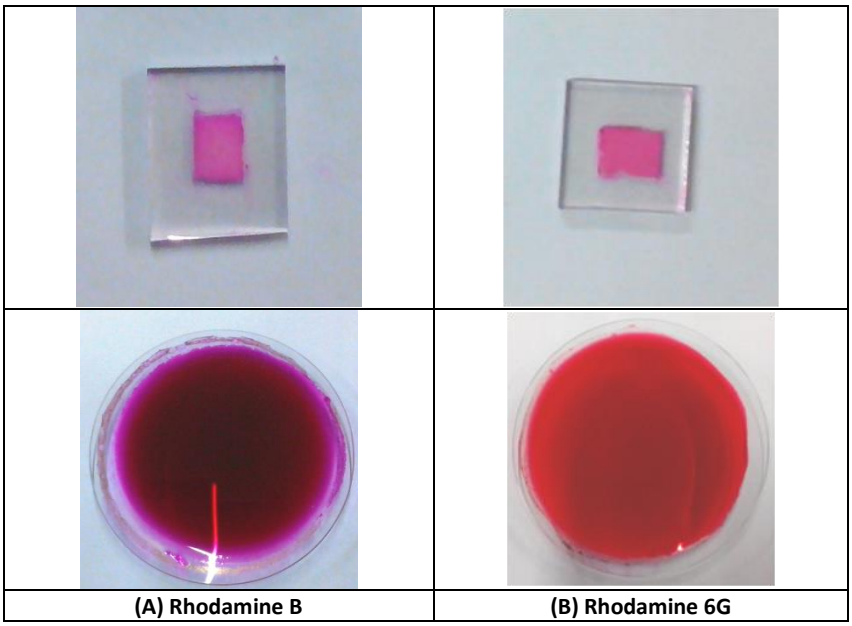

| (A) Rhodamine B | (B) Rhodamine 6G |
|---|---|

**Figure 1: Schematic representation of dye solution in watch glass and substrate coated with $TiO_2$ layer after dye absorption respectively: (A) rhodamine B (B) rhodamine 6G**

ISSN: 0975-8585

At the same time, small $E_g$ value in donor dyes aid in the generation of excitons and increases the efficiency of photoexcitation. Band gap value ($E_g$) is very significant for the generation and recombination of charges. The performance of DSSCs mainly depends on the relative HOMO–LUMO energy levels of the sensitizer. Therefore, efficient electron injection requires the LUMO level of the dye to be higher in energy than the $TiO_2$ conduction band edge, whereas the HOMO of the dye level may lie below the energy level of the electrolyte to allow efficient regeneration of the oxidized dye. The electronic structures, such as FMO ($E_{HOMO}$, $E_{LUMO}$, and band gap $E_g = E_{LUMO}$-$E_{HOMO}$) of dye molecules in DSSC are related to the electron transfer of photo-excitation.

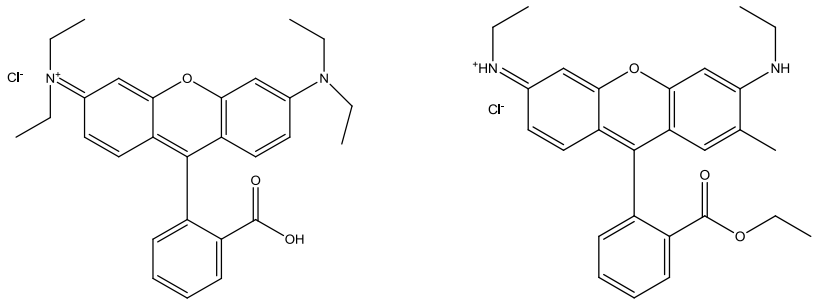


(A) (B)

**Figure 2: Structure of (A) rhodamine B and (B) rhodamine 6G**

**UV-Vis spectrum of dyes**

Figure 3 shows a normalized absorption spectrum of rhodamine B and rhodamine 6G in aqueous solutions. The two broad visible bands at 341 and 590 nm in rhodamine B dye are appearing due to π→π*, n→π* transition respectively. Rhodamine 6G dye shows absorption peak at 348 nm and 501 nm due to π→π*, n→π* transition. The wavelength and the intensity of each absorption peak generally reflect the transition energies and the transition–dipole moments in transitions from the ground state to the singlet-excited states. Intensity of rhodamine B is much higher than rhodamine 6G. An effective sensitizer should absorb radiation over a wide range from the visible region to the near-infrared region and the energy of its electronic excited state supposed to lie energetically above the conduction band of the $TiO_2$ layer. The optical bandgap energy can be determined using the Tauc relation [14-16]. It is a convenient way of studying the optical absorption spectrum of a material. According to the Tauc relation, the absorption coefficient μ for direct band gap material is given by

$$\mu h\nu = A(h\nu - E_g)^n \text{ ----------equ. (1)}$$

Where $E_g$ the band gap, constant A is different for different transitions, (hν) is energy of photon and n is an index which assumes the values ½, 3/2, 2 and 3 depending on the nature of electronic transition responsible for the reflection. The observed values of the optical band gap for rhodamine B was 1.93 eV as shown in fig.4. The calculated optical band gap for rhodamine 6G was 2.15 eV as shown in fig. 5.

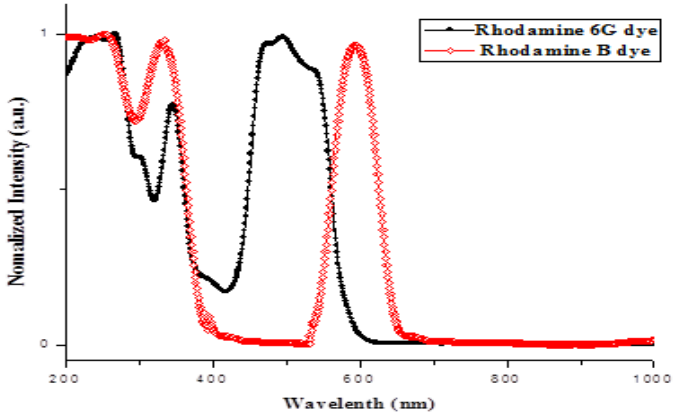


**Figure 3: UV-Vis spectrum of rhodamine B and rhodamine 6G dyes**

ISSN: 0975-8585

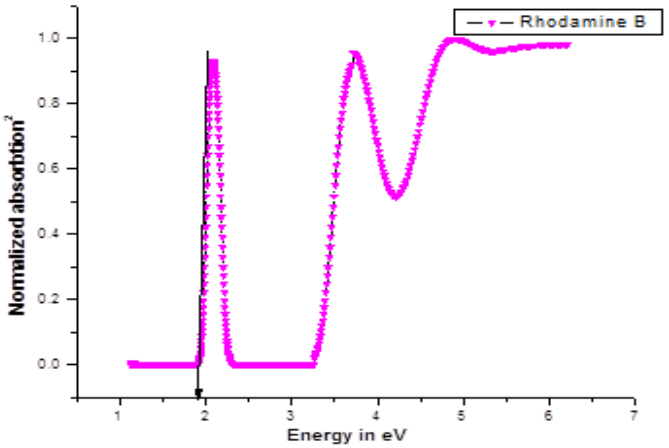


**Figure 4: Optical bad gap of rhodamine B dye**

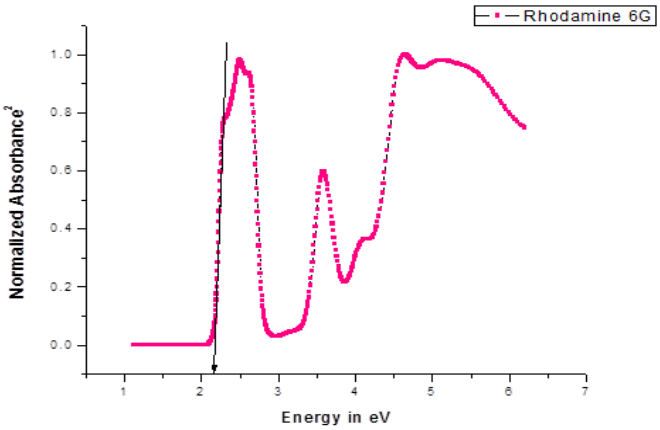


**Figure 5: Optical bad gap of rhodamine 6G dye**

**Thermal properties of dyes**

The TGA and DTA curve were obtained by heating 7.302 and 7.812 mg of rhodamine B and rhodamine 6G respectively, which are represented in Figs. 6-7. TGA plot of rhodamine B shows two steps of mass change with change of temperature. These two steps occurred at 180–230 and 290–340 °C. Upto 180 °C temperature the loss of mass was only 5.28 % i.e. due to evaporation of volatile constituents of dyes. At first step (180-230 °C), the mass loss is 8.4 % correspond to 36.03 g/mol. The most possibility in this step is evaporation of volatile constituents like water of crystallization or self humidity of dye and so $H_2O$ with molar mass 18.1 g/mol was the most likely decomposition product. The change in mass 290 to 340 °C of temperature was found 27.05%. On further heating above 340 °C temperature fast degradation of rhodamine B occurs with huge loss of mass. This decrease in the mass ratio is due to decomposition of low molecular mass constituent ($C_2H_5$) with molar mass 27.24 g/mol and the decomposition of (-NH-) group with molar mass 69.1 g/mol which is responsible for the mass decrease in this range of temperature. The glassy state is characterized by vibration motion of the atoms constituting the compound chain about an equilibrium position. Therefore, the glass transition peak at 200, 209, 223 and 245 °C may apparently be due to the motion of comparatively small kinetic ($C_2H_5$), (-NH-) and ($Cl^-$) side groups.

ISSN: 0975-8585

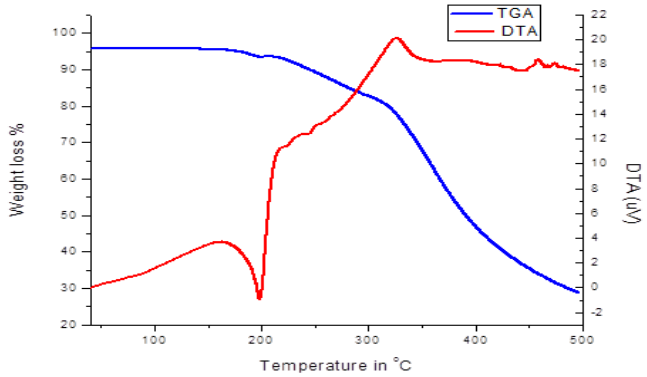


**Figure 6: TGA and DTA of rhodamine B dye**

TGA plot of rhodamine 6G also shows different steps of mass change with temperature. These three steps occurred at 40–115, 170-210 and 310–345 °C. in the first step 40-115 °C temperature the loss of mass was only 3.85 % i.e. due to evaporation moisture and volatile constituents of dyes. At second step (170-210 °C), the mass loss is 11.22 % correspond to 53.74 g/mol. The most possibility in this step is evaporation of volatile constituents like water of crystallization or self humidity of dye and so $H_2O$ with molar mass 18.1 g/mol and may be elimination of HCl. The change in mass 310 to 345 °C of temperature was found 23.25%. On further heating, above 345 °C temperature fast degradation of rhodamine B occurs with huge loss of mass. This decrease in the mass ratio is due to decomposition of low molecular mass constituent ($C_2H_5$) with molar mass 27.24 g/mol and the decomposition of (-NH-) group with molar mass 69.1 g/mol which is responsible for the mass decrease upto 500 °C temperature was found 76.45%. The DTA peaks were present at 115, 190, 205, 315 and 340 °C may apparently be due to the motion of comparatively small kinetic ($C_2H_5$), (-NH-) and ($Cl^-$) side groups. Endothermic peak present at 205 °C shows the phase transfer peak.

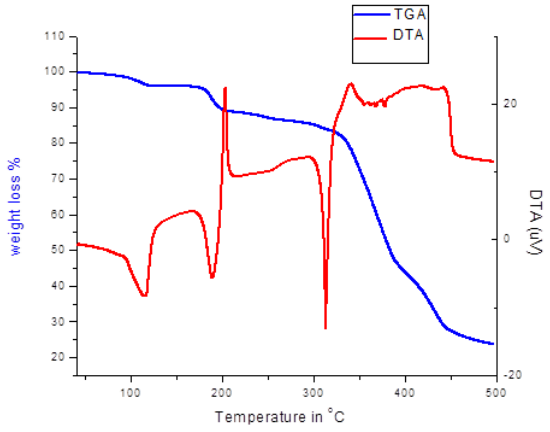


**Figure 7: TGA and DTA of rhodamine 6G dye**

**Photovoltaic properties**

The photovoltaic performance of the fabricated solar cells analysed in terms of cell efficiency (η) [20] and fill factor (FF) [21] is expressed as follows:

$$FF = \frac{V_{max}.J_{max}}{V_{oc}.Jsc}$$

equ. ----------(2)

$$\eta = \frac{V_{oc}.Jsc.FF}{P_{in}} \times 100$$

equ.----------(3)

ISSN: 0975-8585

where $J_{sc}$ is the short-circuit current density (mA/cm$^2$), $V_{oc}$ is open-circuit voltage and $P_{in}$ is incident light power. $J_{max}$ and $V_{max}$ are corresponding to current density maximum and voltage maximum values, respectively, where the maximum power output is given in the J–V curve. In the band gap theory, the difference between the quasi-Fermi level of the $TiO_2$ layer and the electrolyte redox potential determines the maximum voltage generated under illumination. As shown in equ.(4) the open-circuit voltage varies with the iodide concentration because there combination reaction occurs between the electrons on the conduction band of $TiO_2$ and $I_3^-$ (triiodide) [19].

$$V_{oc} = \frac{kT}{q} \ln\left[\frac{\eta \phi_o}{n_o k_{et} [I_3^-]}\right] \qquad \text{equ. ---------- (4)}$$

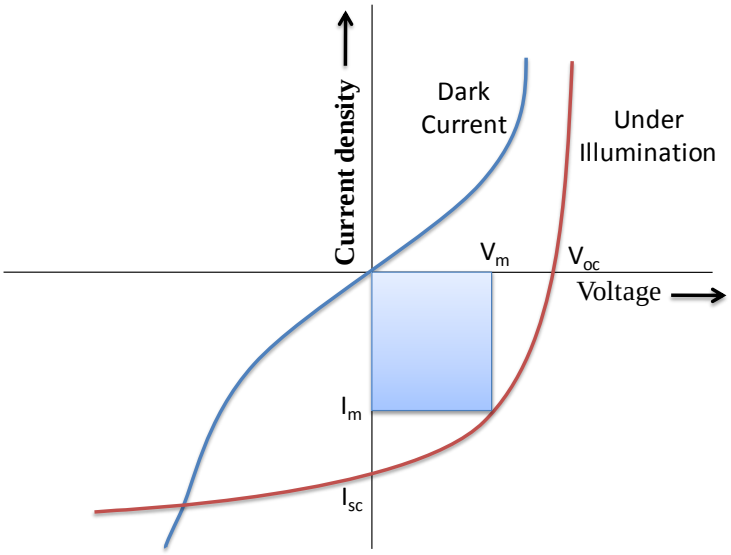


**Figure 8: I-V curve of photovoltaic cell**

where η is the quantum yield of photo-generated electron for the given incident photo flux ($\phi_o$); $n_0$ represents the electron density on the conduction band of $TiO_2$ in the dark, while $k_{et}$ reflects the recombination reaction rate for the given triiodide concentration [$I_3^-$].

**Rhodamine B as sensitizer:** Current density-voltage (J-V) characterization of DSSC based on rhodamine B dye sensitizer is shown in figure 9. The photovoltaic parameters of the fabricated cells are presented in Table 1. The concentration of the redox electrolytes were iodine ($I_2$) (0.01M), potassium iodide (KI) (0.1M), tetramethylquaternaryammonium iodide [$(CH_3)_4NI$] (0.1M), tetraethylquaternaryammonium iodide [$(CH_3CH_2)_4NI$] (0.1M), tetrapropylquaternaryammonium iodide [$(CH_3CH_2CH_2)_4NI$ ] (0.1M) applied in acetonitrile solvent. Open circuit ($V_{oc}$) and short circuit current ($J_{sc}$) were obtained 0.233 V and 5.058 mA/cm$^2$ respectively with redox electrolyte KI-$I_2$. With the use of $(CH_3)_4NI$-$I_2$ redox electrolyte in acetonitrile solvent the $V_{oc}$ (0.247 V) get enhanced and the $J_{sc}$ (4.77 mA/cm$^2$) was found reduced. Highest Voc (0.275 V) value was observed with $(CH_3CH_2)_4NI$-$I_2$ redox electrolyte having $J_{sc}$ (5.267 mA/cm$^2$). Maximum $J_{sc}$ (7.00 mA/cm$^2$) value was found with redox electrolyte $(CH_3CH_2CH_2)_4NI$-$I_2$ having the $V_{oc}$ (0.251 V). The observed efficiency of fabricated solar cell was found in order i.e. $(CH_3)_4NI$-$I_2$< KI-$I_2$<$(CH_3CH_2)_4NI$-$I_2$<$(CH_3CH_2CH_2)_4NI$-$I_2$ with these electrolytic solution.

**Table 1. Photovoltaic properties of of DSSC with rhodamine B dye**

| Electrolytes | $V_{oc}$ | $J_{sc}$ | FF | Efficiency |
|---|---|---|---|---|
| KI-$I_2$ | 0.233 | 5.05 | 0.232 | 2.747 |
| $(CH_3)_4NI$-$I_2$ | 0.247 | 4.77 | 0.194 | 2.291 |
| $(CH_3CH_2)_4NI$-$I_2$ | 0.275 | 5.26 | 0.208 | 3.024 |
| $(CH_3CH_2CH_2)_4NI$-$I_2$ | 0.251 | 7.00 | 0.217 | 3.817 |

ISSN: 0975-8585

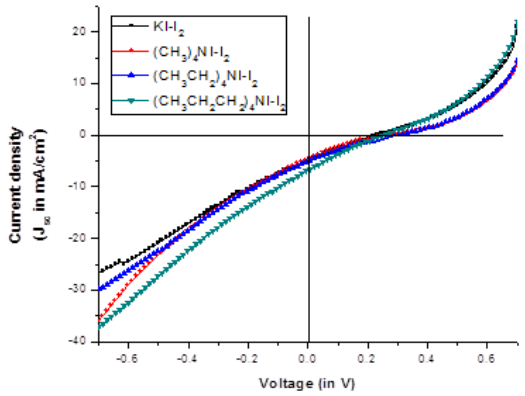


**Figure 9: Current-voltage plot of fabricated solar cell with rhodamine B dye**

**Rhodamine 6G as sensitizer:** The performance of the rhodamine 6G dye as sensitizer for DSSCs was evaluated as shown in table 2. Current density-voltage characterization of DSSC based on rhodamine 6G dye is presented in figure 10. DSSC shows the short circuit current density ($J_{sc}$) of a maximum value 5.27 mA/cm$^2$ with redox electrolyte $(CH_3CH_2CH_2)_4NI$-$I_2$ and a minimum value 03.02 mA/cm$^2$ with $(CH_3)_4NI$-$I_2$ electrolyte. The open circuit voltage ($V_{oc}$) ranges between 0.227 V for fabricated cell with $(CH_3)_4NI$-$I_2$ redox electrolyte and 0.346 V with $(CH_3CH_2CH_2)_4NI$-$I_2$ redox electrolyte. The fill factor of the fabricated cells changed from 0.164 to 0.264. The lowest fill factor was observed in cell with $(CH_3)_4NI$-$I_2$ electrolyte whereas the highest fill factor was obtained with KI-$I_2$. The highest efficiency of cell was obtained with $(CH_3CH_2)_4NI$-$I_2$ redox electrolyte where the lowest efficiency was with $(CH_3)_4NI$-$I_2$ electrolyte. The overall order of performance of DSSC increases with use of these redox electrolytes i.e. $(CH_3)_4NI$-$I_2$< KI-$I_2$-$I_2$<$(CH_3CH_2CH_2)_4NI$-$I_2$<$(CH_3CH_2)_4NI$.

Photovoltaic properties of fabricated DSSCs were obtained by the addition of inorganic iodides such as KI and organic iodides like tetraalkylquaternaryammonium iodides ($R_4NI$) where R = $CH_3$, $C_2H_5$ and $C_3H_7$) on the photovoltaic performance of the DSSC. From $CH_3$ to $C_3H_7$ cation, the efficiency of solar cell increased in the cell performance. The reason for this characteristic behavior may be correlated with ionic radius of the different cations [20]. The $V_{oc}$ of the DSSC in quaternary ammonium iodide-iodine redox electrolyte was derived from the energy gap between the conduction band level of the $TiO_2$ and $I^-/I_3^-$ redox potential of alkyl cations. As a result of this, the conduction band of the $TiO_2$ shifted negatively from $CH_3$ to $C_3H_7$, leading to the increase of the $V_{oc}$ and the vice-versa [21].

**Table 2. Photovoltaic properties of DSSC with rhodamine 6G dye**

| Electrolytes | $V_{oc}$ | $J_{sc}$ | FF | Efficiency |
|---|---|---|---|---|
| KI-$I_2$ | 0.267 | 3.66 | 0.264 | 2.58 |
| $(CH_3)_4NI$-$I_2$ | 0.227 | 3.02 | 0.164 | 1.131 |
| $(CH_3CH_2)_4NI$-$I_2$ | 0.346 | 3.07 | 0.319 | 3.408 |
| $(CH_3CH_2CH_2)_4NI$-$I_2$ | 0.261 | 5.27 | 0.240 | 3.322 |
| | | | | |

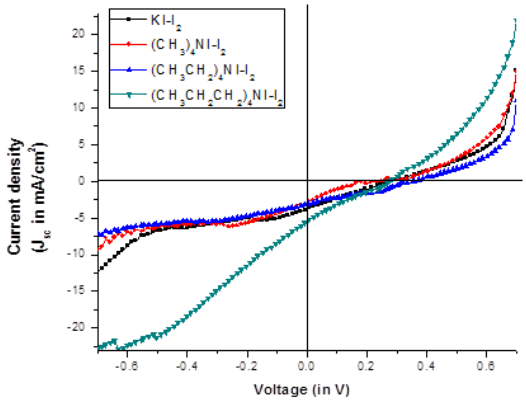


**Figure 10: Current-voltage plot of fabricated solar cell with rhodamine 6G dye**

## CONCLUSION

Nano-titania based DSSC prepared with FTO glass had been successfully analyzed with the effect developed with the use of rhodamine B and rhodamine 6G dyes. These commercial dyes helped in the spectral response of $TiO_2$ electrode that could be extended well into the visible region (up to 700 nm wavelength). Absorption spectra of these dyes adsorbed on $TiO_2$ electrode provided clear evidence for its purpose of photosensitizers. Best performance out of all fabricated devices was reported in case of rhodamine B when used as sensitizer with $(CH_3CH_2CH_2)_4NI$-$I_2$ redox electrolyte. These dyes exhibited excellent properties such as better anchorage to the $TiO_2$ surface, Thermal stability, chemical stability and wide visible spectrum which make them promising candidates for use as sensitizers in DSSCs. Although, these DSSC showed low photovoltaic performance in comparison to inorganic dye, however still owning to their easy and efficient low-cost fabrication.

## REFERENCES


[1] Hasan MA, Sumathy K. Renewable and Sustainable Energy Reviews. 2010;14(7);1845–59.
[2] http://www.sunenergy.com.au/pdf/CLSA1.pdf
[3] Shah A. Thin-Film Silicon Solar Cells. EPFL Press. Switzerland 2010.
[4] Chapin DM, Fuller CS, Pearson GLJ. J Applied Physics 1954;25;676.
[5] King RR, Law DC, Edmondson KM, Fetzer CM, Kinsey GS, Yoon H, Krut DD, Hermer JH, Sherif RA, Karam NH. Advances in Optoelectronics 2007:Article ID 29523.
[6] Goetzeger A, Hebling C. Solar Energy Material Solar Cells 2000;62;1-19.
[7] O'regan B, Grätzel M. Nature 1991;353;737-740.
[8] Spanggaard H, Krebs FC. Solar Energy Materials & Solar Cells 2004, 83, 125-146.
[9] Bube RH, Photoconductivity of Solids, Wiley, New York, 1960;169.
[10] Chamberlain GA. Solar Cells 1983;8;47-83.
[11] Kanicki J, Skotheim TA. Handbook of conducting polymers, Vol. 1, Marcel Dekker, New York, 1985.
[12] Tang CW. J Applied Physics Letter 1986;48;183-185.
[13] Yan C, Zharnikov M, Gölzhäuser A, Grunze M. Langmuir 2000;16 **;**6208-6215.
[14] J. Tauc, in: F. Abeles (Ed.), The Optical Properties of Solids. 1972;37, North-Holland, Amsterdam.
[15] Nahass MME, Farag AM, Abd El-Rahman KF, Darwish AAA. Optics Laser Technol 2005;37;513-523.
[16] Yakuphanoglu F, Arslan M. Optical Materials 2004;27;29-37.
[17] Shockley W, Queisser HJ. J Applied Physics 1961;32:510-519.
[18] Green MA. Solid-State Electronics 1981;24:788 - 789.
[19] LanZ, Wu J, Wang D, Hao S, Lin J, Huang Y. Solar Energy 2007; 81(1): 117–122.
[20] Yao Liu, Anders Hagfeldt, Xu-Rui Xiao, Sten-Eric Lindquist. Solar Energy Materials Solar Cells 1998;55;267-281
[21] K. Hara, T. Horiguchi,T. Kinoshita, K. Sayama, H. Arakawa. Solar Energy Materials Solar Cells 2001;70;151-161.